50th AIAA Aerospace Science Meeting, Nashville, TN, USA, 9-12 January 2012

Hotwires in pressurized, cryogenic environment - It works!

Harald Quix[1], Jürgen Quest[2]
European Transonic Windtunnel GmbH, 51147 Cologne, Germany

The European Transonic Windtunnel is an unique aerodynamic testing facility also for laminar flow investigations at flight Reynolds numbers. To analyze the laminar flow results additional information about the actual flow quality are essential. Therefore ETW is investigating the possibility of using the hotwire measurement technique for an application under its cryogenic and pressurized conditions. Although the hotwire technique is widely used and very common to assess flow qualities in wind tunnels the operation under the harsh conditions of a cryogenic wind tunnel facility is rare and very poorly documented. Therefore ETW has performed a test campaign in its pilot facility (PETW) to investigate and understand the basic behavior of hotwires over the complete operating envelope of ETW /PETW. The present paper summarizes the results of this test campaign and documents why the hotwire measurement technique is applicable under pressurized and cryogenic conditions.

Nomenclature

d	wire diameter	[m]
E_{br}	anemometer bridge voltage	[V]
$f(x)_{corr}$	correction function for influence parameter x	[-]
f	frequency	[Hz]
k	thermal conductivity	$[\mathrm{W/(Km)}]$
Nu	Nusselt number	[-]
Ma	Mach number	[-]
P_{tot}	total pressure	[Pa]
P_{stat}	static pressure	[Pa]
Re	Reynolds number	[-]
R_c	cable resistance	$[\Omega]$
R_{fix}	fixed resistance	$[\Omega]$
R_o	overheat setup resistance	$[\Omega]$
R_{sup}	support resistance	$[\Omega]$
R_w	wire resistance	$[\Omega]$
T_{tot}	total temperature	[K]
T_{stat}	static temperature	[K]
T_{rec}	recovery temperature	[K]
T_w	wire temperature	[K]
Tu	turbulence level	[-]
U_{flow}	tunnel flow velocity	[m/s]
U	flow velocity perpendicular to wire	[m/s]
$\overline{U}$	mean flow velocity	[m/s]
$\widetilde{u}, \widetilde{v}, \widetilde{w}$	velocity fluctuations	[m/s]
ρ	density	$[\mathrm{kg/m^3}]$
γ	overheat ratio	[-]
ν	kinematic viscosity	$[\mathrm{m^2/s}]$
η	dynamic viscosity	$[\mathrm{Ns/m^2}]$

[1]Aerodynamic and Data Processing Engineer, AIAA member
[2]Chief Aerodynamicist, AIAA associated fellow

I. Introduction

The European Transonic Windtunnel is one of the world leading aerodynamic test facilities and the worldwide unique tunnel for laminar flow investigations at flight Reynolds numbers. Therewith it plays a major role in the development chain of future aircraft with a laminar wing design. In ETW first laminar flow tests were successfully performed during the last years. While the laminar flow regions are measured by temperature sensitive paint (TSP) the flow fluctuations are mainly measured by dynamic pressure measurements. For an exact interpretation of the TSP results additional information about the flow quality are essential. These additional information can be provided by the hotwire measurement technique measuring unsteady flow disturbances based on the principle of heat transfer. For standard applications at ambient pressure, ambient temperature and subsonic speeds, the hotwire anemometry technique is very well documented and a lot of results are available. But leaving these standard conditions in any direction by changing pressure, temperature or going to transonic speeds, the available literature is diminished and the system setup and result analysis becomes more and more challenging. Hence, before using hotwires to support laminar flow test campaigns it is necessary to understand the basic behavior of hotwires under the changing flow conditions of ETW.

Therefore ETW performed a test campaign in its pilot facility (PETW) offering the same operational envelope as the larger ETW but having a much better accessibility combined with lower costs. The overall objective of this test campaign was to figure out if the hotwire measurement technique is applicable in a pressurized and cryogenic environment and produces reasonable results under these conditions.

Because PETW has the same unique ability to separate between compressibility, friction and deformation effects by controlling the parameters temperature, pressure and Mach number independently, it is possible to isolate the different influencing parameters on the heat transfer of a hotwire. This leads to the opportunity to reach a comprehensive understanding of the hotwire behavior under pressurized and cryogenic conditions, being essential for an application of the technique in future test campaigns, where different relevant parameters may change simultaneously. Hence, one goal was to determine a correction function allowing to compensate the different disturbing effects in a way, that the output can be matched to the calibration curve measured under ambient conditions outside the tunnel.

The following chapters summarize the objectives, explain the chosen test program and describe the special test setup, defined by the constructional constraints of ETW. While in a former paper[14] the focus was mainly on the static hotwire output and the correction terms, this paper will concentrate on the global correction function and the final hotwire outcome, the determination of flow disturbances.

Summarizing the paper will show the hotwire measurement technique as a suitable way to perform flow quality assessments under pressurized and cryogenic conditions up to the transonic speeds of a high Reynolds number facility like ETW.

II. Test Objectives

The overall objective of the test campaign in PETW was the validation of the hotwire measurement technique under the pressurized and cryogenic conditions of ETW and PETW. To reach this goal, several questions had to be answered. An obvious question was the survivability of the thin wires under the harsh conditions and transonic speeds. If the wires would not survive several test runs, the measurement technique is not applicable at all. The second question was, if the results are reproducible, meaning the same test condition would give the same results. This is also essential for the application in ETW.

Beside these two general questions, the investigation of the different influencing parameters was a challenging, but necessary part of the test to reach another test objective. In general it is possible to perform an in situ calibration of hotwires in the ETW/PETW, because all flow parameters are well known, but in the practical application this is impossible because of time and cost reasons. Therefore the favored approach would be a calibration outside the tunnel using a standard calibration unit and then take this calibration combined with determined correction functions to apply it over the complete operational envelope of ETW/PETW. The PETW campaign should clarify if such a demanding approach is feasible at all. Finally, the developed data reduction chain should answer the basic question if the hotwire measurement technique is applicable for flow quality assessment in ETW/PETW.

III. Test setup

A. Test facility - PETW

The test campaign was performed in the pilot facility (PETW) of the European Transonic Windtunnel, which originally has been built to test and validate the cryogenic wind tunnel technology before finally designing the larger European Transonic Windtunnel. Still today PETW is used as test facility to adapt and approve existing measurement techniques for cryogenic conditions and develop and validate new hardware components before using them in ETW.
The PETW is scaled down by 1:8.8 compared to ETW. Although PETW and ETW are not built identically, they cover the same operational range with respect to temperature, Mach number and pressure. The main difference is the insulation type, where PETW has an external insulation of a box type, while ETW is fully insulated internally. The second major different between the two tunnels is their control system. While ETW has an complete automatic control system, allowing to keep the three flow parameters perfectly constant, PETW is mainly controlled manually, resulting in less accurate and less stable conditions.

B. Hotwire Setup

For the use in ETW the standard hotwire anemometry setup has to be adapted to the special requirements of a cryogenic test facility. The wide temperature range between 110 [K] and 300 [K] is the most obvious difference compared to conventional wind tunnels. This temperature difference results in some related aspects which have to be taken into account. One of the most challenging aspect is the long distance between the test section under cryogenic conditions and the measurement cabin at ambient temperature. Fig. 1 displays the arrangement of ETW's movable model cart and shows the temperature barrier between cryogenic part and the ambient part.

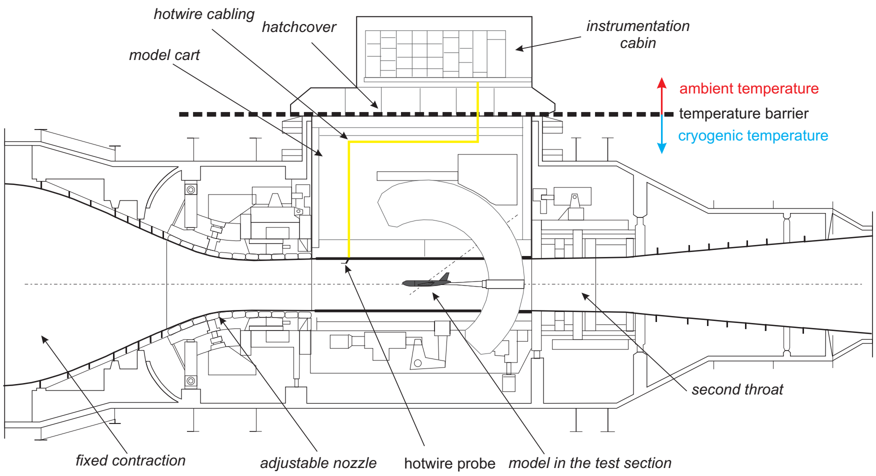

Fig. 1. ETW side view with model cart

This distance requires 25 meters of cryogenic suitable cables. For this purpose a CAT-5 cable was successfully validated under cryogenic conditions. The cable has four twisted pairs of wires, hence, exactly matching the required number. Two pairs are required for the chosen double hotwire probe and the two other pairs are necessary to compensate for the changing cable resistance by shortcutting the wires at their ends using a DANTEC shortcut probe. This compensation setup is essential because of the floating cable resistances caused by the cable passing the tunnel isolation from the cryogenic temperature side to the instrumentation cabin at ambient temperature. To simulate the ETW setup the same cable arrangement was used for the PETW test campaign.

The used hotwire probes are a DANTEC miniature x-wire probes made of stainless steel. To increase the survivability of the wires, the original wires were replaced by 5 $[\mu m]$ thin gold-plated tungsten wires with a little slack between the prongs to compensate the thermal contraction. The two wires of such an x-wire probe form an angle of 90 deg with each other and are inclined by 45 deg to the mean flow direction (Fig. 2), so that they are capable to measure two-dimensional unsteady flow fields. For the PETW test one of the four procured probes was installed at the center of the top wall outside the boundary layer, while the compensating shortcut probe was mounted mirrored on the bottom wall (Fig. 3).

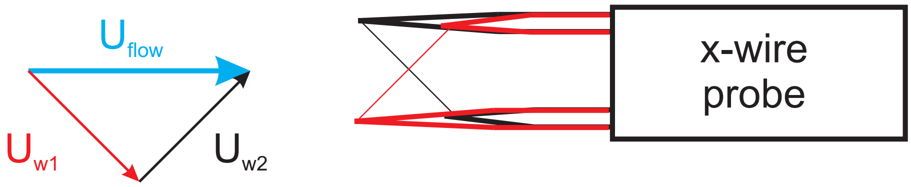

Fig. 2. x-wire probe layout and used velocity definition

The used anemometer system is a DANTEC StreamLine Research Constant Temperature Anemometer system with two installed anemometer units operated in a symmetrical 1:1 bridge configuration. This configuration is needed because a of the long cables and the described necessity to compensate their resistance. To adjust the overheat ratio of the hotwires, external precision potentiometers were used. The resulting bridge layout is presented in Fig. 4.

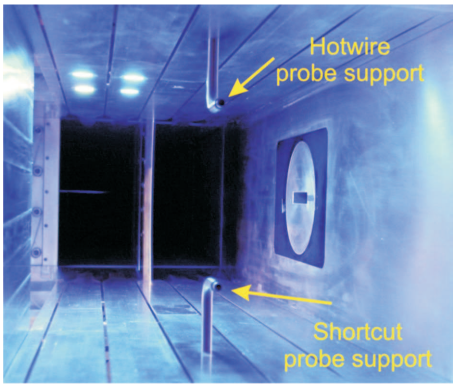

Fig. 3. PETW probe installation

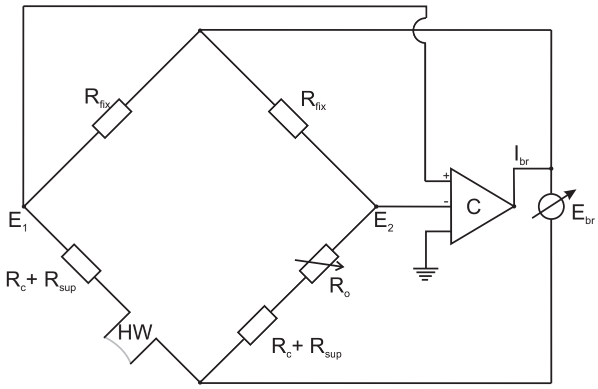

Fig. 4. Anemometer bridge layout

The DANTEC anemometer is connected to a high speed data acquisition system, recording the DC and AC voltage components of the two hotwires with 100 kHz, and to the tunnel data acquisition system monitoring the tunnel flow parameters and temperatures.

IV. Test program

The test campaign was started with a subsequent calibration of all four probes at ambient environment outside PETW using the standard DANTEC calibration unit. Afterwards a similar calibration was performed in PETW using the standard PETW control philosophy to run the tunnel at constant total pressure and temperature and to vary the Mach number. The comparison of the two calibrations pointed out, that the standard control method of PETW is not suitable for the hotwire test campaign because of changing density simultaneous with Mach number. Hence, the final test program was outlined in a way, that only one parameter was changed at the time. The variable parameters are velocity (Mach number), temperature, density and the overheat ratio of the hotwires.
The test program was separated in three temperature levels. At each temperature level the density and the overheat ratio were varied in three steps and at each of these test points the Mach number and therewith the velocity was increased in several steps from Ma=0.0 [-] to Ma=0.9 [-] (Fig. 5).
This test program nearly covered the complete operational envelope of ETW/PETW (excluding the supersonic part) and allows the investigation of the different influences to find the aimed correction functions for them. Fig. 6 shows the test points of the final test program as function of temperature and density. The test program was performed twice to increase the available data set, to get used to the hotwire measuring procedures and to allow statements about the survivability and repeatability. Unfortunately, due to problems with the high speed data acquisition system the set of unsteady data is incomplete for the first test entry.

Ma = 0.00 [-]
Ma = 0.15 [-]
Ma = 0.20 [-]
Ma = 0.30 [-]
Ma = 0.40 [-]
Ma = 0.50 [-]
Ma = 0.60 [-]
Ma = 0.70 [-]
Ma = 0.80 [-]
Ma = 0.90 [-]

Fig. 5. Mach numbers tested at each test point of Fig. 6

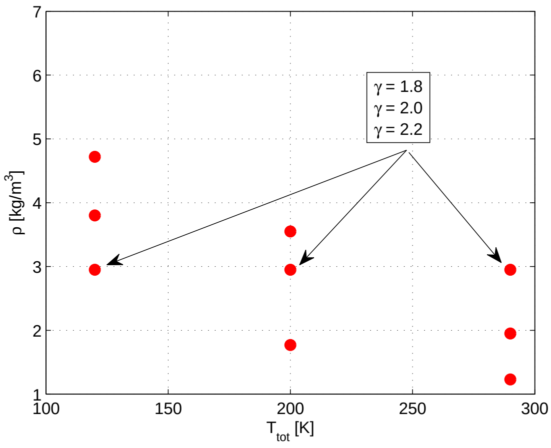

Fig. 6. Test points as function of temperature and density

V. Results

During the test campaign a huge amount of data was collected. The following sections give an overview about the outcomes of the test. For a better understanding the results are subdivided in steady and unsteady results as well as in general findings. The steady results and first correction terms were already discussed in detail in a former paper,[14] so that this paper concentrates on the expansion towards a global correction function and on the unsteady results.

A. Reference Calibration

The first calibration of the hotwire probe was performed using a standard DANTEC calibration unit. This unit is able to vary the flow velocity and therewith allow to determine the correlation between flow velocity and bridge output voltage. The result of this calibration is shown in Fig. 7, representing a monotonically increasing curve offering the unique correlation between hotwire output signal and flow velocity according to the King's law.
This calibration curve is used as reference for the results of the PETW test with the goal to match all PETW results to this calibration. If this would be successful, it would be a very efficient way of using hotwires in ETW /PETW because additional time consuming and cost intensive calibrations in the test section could be avoided.
Taking a closer look to the flow parameters of the calibration unit, it has to be mentioned that there is a second changing parameter, the density. Although the calibration unit is used at ambient air conditions with an open jet flow and therewith the static pressure remains constant for all velocities, the static temperature decrease as function of an increasing Mach number results in a rising density. Therefore it is important to correct also this reference calibration curve for changing density using the findings of the density variations in PETW.

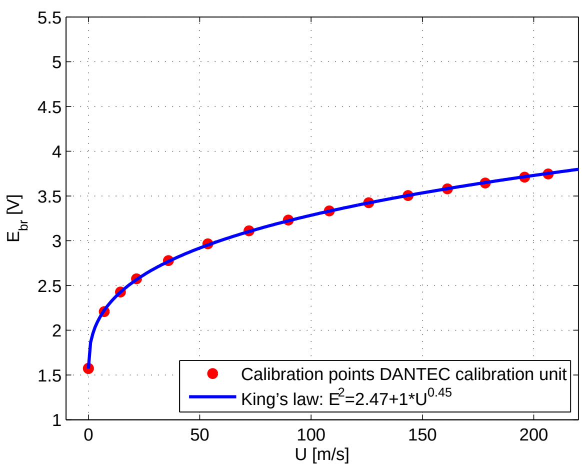

Fig. 7. Test points as function of temperature and density

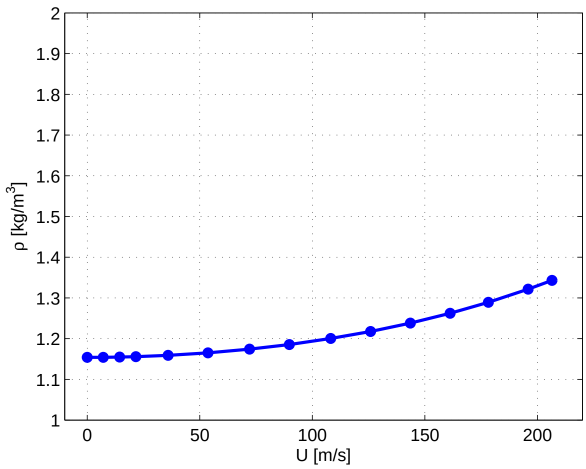

Fig. 8. Density characteristic over calibration range

B. Steady Results

Velocity

The velocity is the main measurement variable for hotwire measurements because it is directly linked to the bridge output voltage. The flow velocity is a function of Mach number, one of the basic variable test parameters in wind tunnels campaigns. The bridge output voltage depending on flow velocity is the main calibration parameter of a hotwire, which is required to asses flow quality. Hence, the velocity can be treated as an independent parameter, not necessary to correct its influence.
In opposite to the conditions during the reference calibration, PETW allows to control the flow parameters independently, so that the test was performed with Mach number and therewith velocity as the only changing parameter. Fig. 9 shows the bridge output voltage as function of the tunnel Mach number at three different temperature levels. Although measured at the same Mach number the resulting curves have significant differences. On one side this is caused by the decreasing flow velocity with falling temperature due to the decreasing speed of sound. On the other side it is obvious that the same flow velocity does not produce the same bridge output signal (Fig. 10), concluding that there are additional effects, which will be discussed in the next sections.
The figures 9 and 10 show the measured data points fitted according to the King's law. Visible is a difference between the fit and the measured values at the highest Mach number. This drop in bridge voltage at high Mach numbers was already observed by Spangenberg[16] and explained by the different temperature loading of the wire, which can be quantified by the ratio $(\mathrm{T_w} - \mathrm{T_{rec}})/\mathrm{T_{stat}}$. Here, this effect seems to be more effective at ambient temperatures and decreased towards lower temperatures.

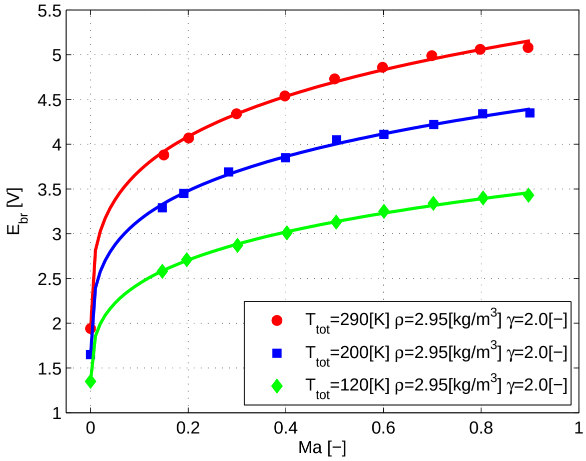

Fig. 9. Bridge output as function of Mach number

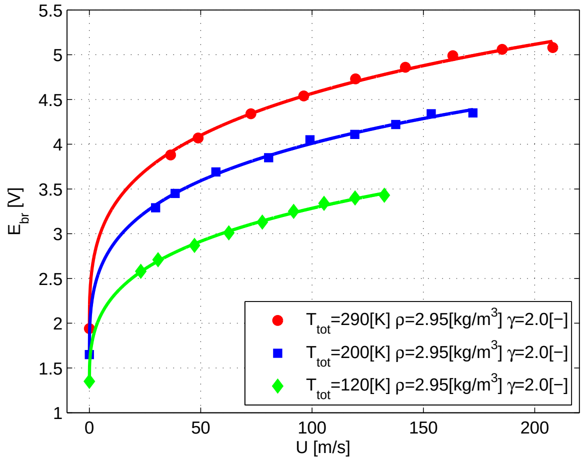

Fig. 10. Bridge output as function of velocity

Density

As expected, the influence of a changing density was found to be similar at different temperature levels, because of changing the convection conditions in the same way. Hence, the data were used to extract a density correction function, determined to:

$$f(\rho)_{corr} = (\frac{\rho_{ref}}{\rho})^{0.23} \tag{1}$$

Exemplary Fig. 11 shows the density influence and Fig. 12 the corrected data for a temperature of 120 [K] and a reference density of $\rho_{ref} = 2.95[kg/m^3]$.

Overheat Ratio

The overheat ratio is specifying the wire temperature and therewith has a direct effect on the heat transfer to the surrounding flow. Also for the overheat ratio it can be stated, what its influence can be separated from other influences and hence, it could be corrected. The correction here was found to:

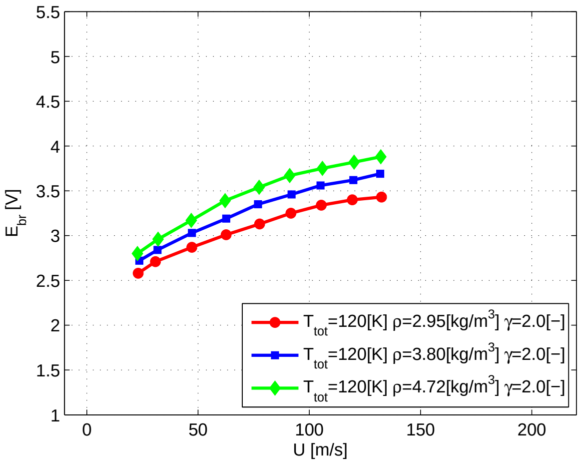

Fig. 11. Density influence at $\mathbf{T_{tot} = 120[K]}$

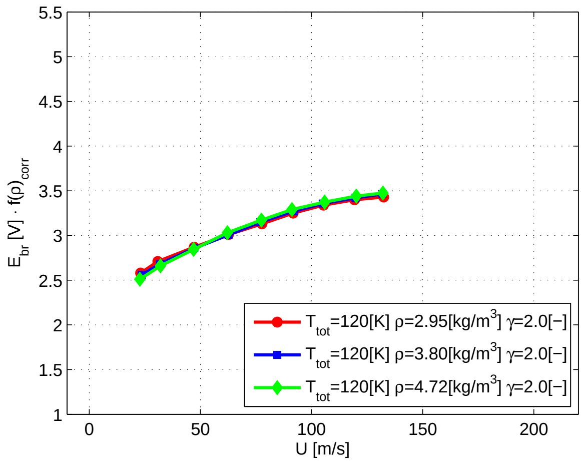

Fig. 12. Density influence at $\mathbf{T_{tot} = 120[K]}$ corrected

$$f(\gamma)_{corr} = (\frac{\gamma_{ref}}{\gamma})^{0.6} \tag{2}$$

Fig. 13 presents the influence of different overheat ratios at 200 [K] while Fig. 14 shows the results of the applied correction with $\gamma_{ref} = 2.0[-]$

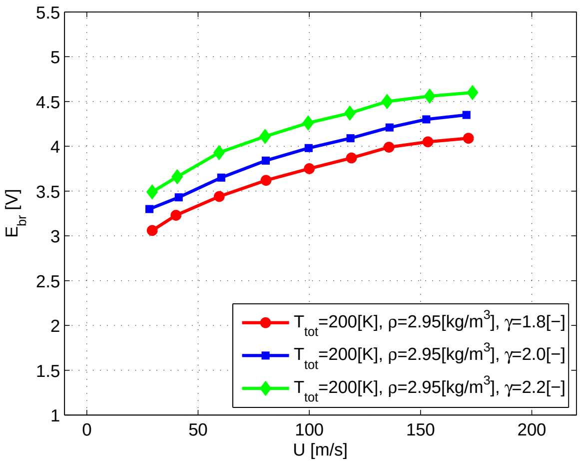

Fig. 13. Overheat ratio influence at $\mathbf{T_{tot} = 200[K]}$

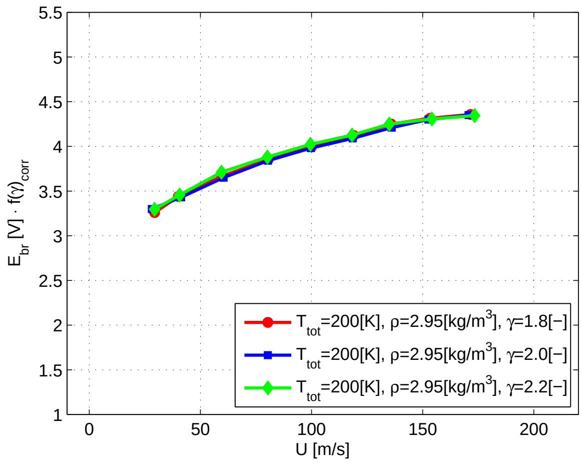

Fig. 14. Overheat ratio corrected $\mathbf{T_{tot} = 200[K]}$

Temperature

The investigation of temperature influence and its correction turned out to be the most challenging task caused by the resistances changing with temperature and the partly warm and partly cold cable. Obviously the resistances directly influence the bridge setup and its output signal, so it is important to know the actual values. For the present test campaign the resistances were only measured at the beginning of each temperature level and then assumed to be constant over the run. This assumption turned out to be not very accurate and caused some additional question marks during the analysis. Therefore it must be stated, that it would have been much better to measure the resistances as often as possible, at least after each Mach number sweep. In future test campaigns it should be done always during the measurement of balance zeros.
Hence, using the data for a sufficient temperature correction is quite difficult. Because all resistances are decreasing with falling temperature the observed drop in bridge voltage can not be interpreted as pure temperature effect on the heat transfer but as effect following the electrical laws. Assuming a constant anemometer current to power the bridge, a lower bridge resistance will cause a lower bridge output voltage, observable in Fig. 15. To correct for this

electrical effect it is necessary to reference the bridge resistances to a reference case using the following correction function:

$$f(T)_{corr_a} = \frac{R_{w_{ref}} + R_{c_{ref}} + R_{sup_{ref}} + R_{fix}}{R_w + R_c + R_{sup} + R_{fix}} \tag{3}$$

To make this temperature correction also applicable for runs with different overheat ratios, it is necessary to cancel out the overheat setup, because this influence is already corrected by the correction function $f(\gamma)_{corr}$. The overheat value is only affecting the wire resistance and therewith can be canceled out by multiplying the wire resistance by the overheat ratio, resulting in the following correction term:

$$f(T)_{corr_b} = \frac{R_{w_{ref}} + R_{c_{ref}} + R_{sup_{ref}} + R_{fix}}{R_w \cdot \frac{\gamma}{\gamma_{ref}} + R_c + R_{sup} + R_{fix}} \tag{4}$$

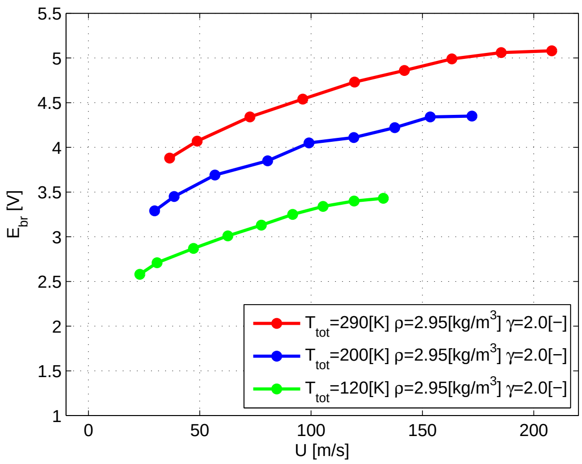

Fig. 15. Temperature influence at $\gamma = 2.0[-]$

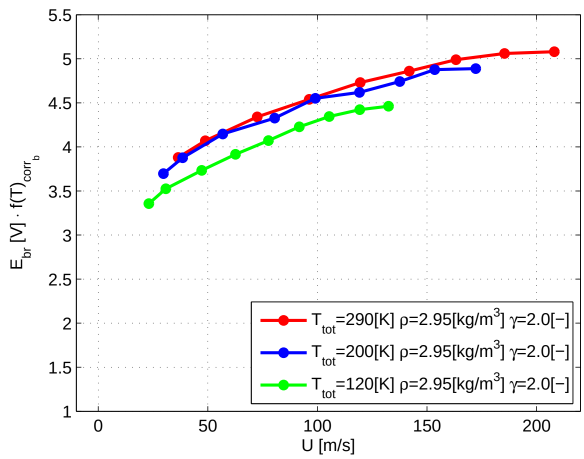

Fig. 16. Temperature influence at $\gamma = 2.0[-]$ corrected for electrical bridge setup

The result of the applied correction is illustrated in Fig. 16 with the ambient run as reference case. It is visible that the correction goes in the right direction but still does not reach a good match. So far the reason for the remaining offset is unknown, it could be a real temperature effect, for example caused by different temperature loadings of the wire, or an additional change within the anemometer setup, exemplary a different current. The fact, that the offset is slightly different for the two wires of the probe could be a hint to be not a pure temperature effect but a difference in the anemometer setup. A more detailed analysis with additional temperature levels is required to clarify if the offset is a physical temperature phenomena and more driven by an electrical effect.
Despite the unknown reason of the offset it is possible to correct it by multiplying the bridge output voltage by a constant value depending on temperature. Because only three different temperature levels are available, the confidence level of this correction is low and the correction has to be proven by test results at additional temperature levels. Using the data of both wires the correction term was found to be a second order polynomial, resulting in the following overall temperature correction:

$$f(T)_{corr} = \frac{R_{w_{ref}} + R_{c_{ref}} + R_{sup_{ref}} + R_{fix}}{R_w \cdot \frac{\gamma}{\gamma_{ref}} + R_c + R_{sup} + R_{fix}} \cdot (1 - 0.0162 \cdot \frac{290[K]}{T} + 0.0172 \cdot (\frac{290[K]}{T})^2) \tag{5}$$

Figures 17 and 18 show the good agreement of the finally temperature corrected test results. Using a different polynomial for each of the wires would lead to even better results, but would exclude that the correction is based on a general temperature effect.

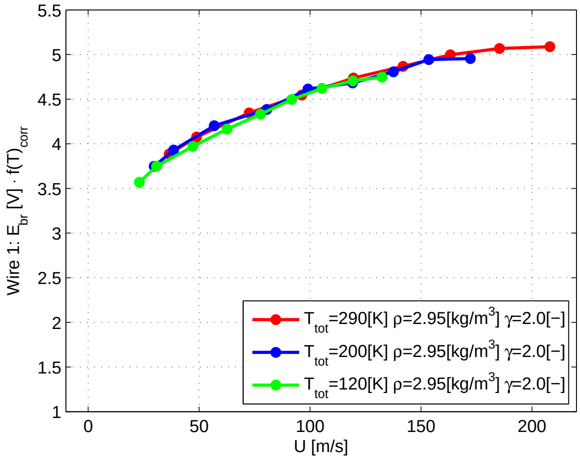

Fig. 17. Temperature influence wire 1 at $\gamma = 2.0[-]$ finally corrected

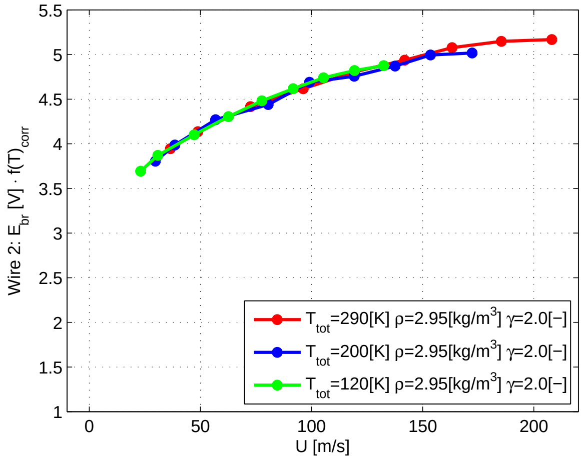

Fig. 18. Temperature influence wire 2 at $\gamma = 2.0[-]$ finally corrected

C. Global Correction Function

As already mentioned one objective for investigating the different influence parameters and extracting correction functions was to find a way of tracing a measurement at any tunnel condition back to the initial calibration performed outside the tunnel. Therefore the different correction terms presented in the previous chapters have to be combined to a global correction function. Because the different correction terms are independent of each other, they do not affect each other, so that the global correction function can be composed by a simple multiplication of the single correction terms:

$$f(\rho, \gamma, T)_{corr} = f(\rho)_{corr} \cdot f(\gamma)_{corr} \cdot f(T)_{corr} \tag{6}$$

Fig. 19 and Fig. 20 show the corrected results of both wires for all measured test points applying the following reference conditions to the correction terms:

- $\rho_{\mathrm{ref}} = 1.25[\frac{\mathrm{kg}}{\mathrm{m}^3}]$
- $\mathrm{T}_{\mathrm{ref}} = 290[\mathrm{K}]$
- $\gamma_{\mathrm{ref}} = 2.0[-]$

The plots confirm the applicability of the global correction term, showing a good match for all measured point of the PETW test campaign with the reference case.
Because often the bridge voltage and velocity are converted into the dimensionless values represented by Nusselt and Reynolds numbers, the figures 21 and 22 present the results of the fully corrected data in these dimensionless values. The values are based on the corrected bridge output voltage and flow quantities of the reference case, using the following equations:

$$Nu = E_{br}^2 \cdot \frac{R_w}{(R_w + R_c + R_{sup} + R_{fix})^2} \cdot \frac{1}{\pi \cdot l \cdot k \cdot (T_w - T_{tot})} \tag{7}$$

$$Re = \frac{U \cdot d}{\nu_{Ref}} \tag{8}$$

As expected the plots show the same good match as the figures 19 and 20 and the fit using the King's law results in the identical exponent, which is important for the analysis of the unsteady data. The quality of the global correction function can be quantified by the residual mean square error of all data points compared to the applied fit, which is around 0.001 for both wires.

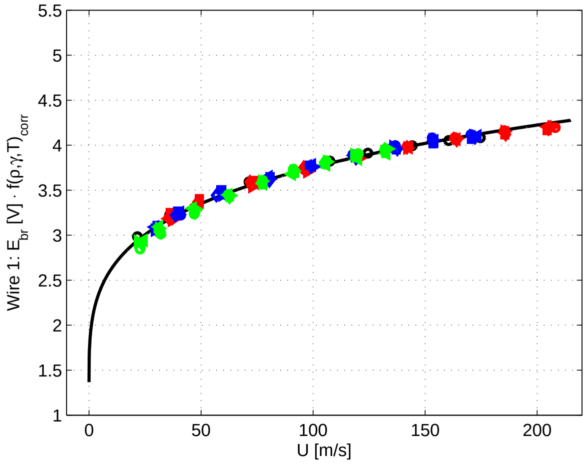

Fig. 19. Results of wire 1 for all test cases with the global correction function applied

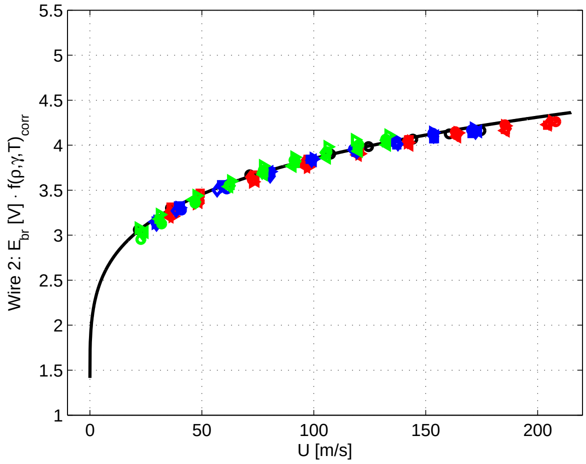

Fig. 20. Results of wire 2 for all test cases with the global correction function applied

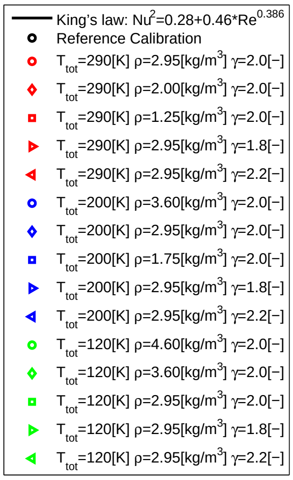

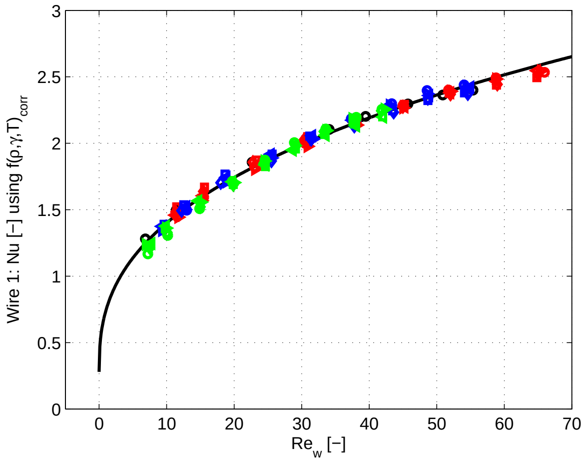

Fig. 21. Dimensionless results of wire 1 for all test cases with the global correction function applied

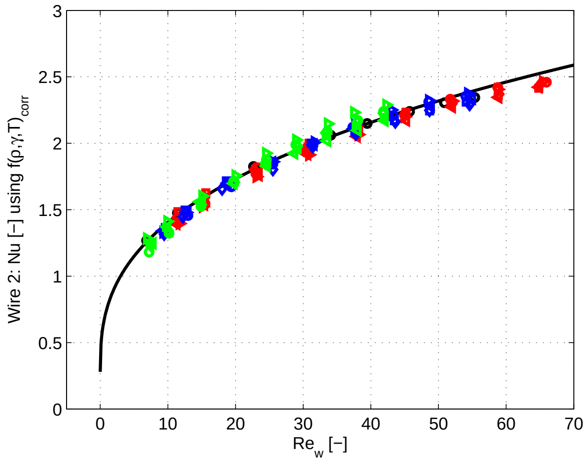

Fig. 22. Dimensionless results of wire 2 for all test cases with the global correction function applied

D. Unsteady Results

While the steady results were used to extract a calibration curve, which is necessary to interpret the unsteady results, these unsteady data are containing the wanted information about flow quality and flow disturbances. The ability to measure highly dynamical flow characteristics with a direct link between the physical phenomena and the output signal is the biggest advantage of the hotwire measurement technique. The presented results show, that this benefit is also existing under cryogenic conditions.

For each test condition in the DANTEC calibration unit as well during the PETW test campaign unsteady data were recorded using a high speed data acquisition system. For the recording a sampling frequency of 100 kHz was applied over a period of 5 seconds with an additional low pass filter at 40 kHz.

Spectral Analysis

Spectral analysis are used to analyze and identify the magnitude and frequency of disturbances. As starting point of this analysis the data of the four procured DANTEC x-wire probes measured within the DANTEC calibration unit were investigated. Figures 23 and 24 give an extracted sample of the measured power spectral densities (PSD) for both wires of two probes at the maximum Mach number. The PSD characteristic versus frequency is quasi identical up to 7 [kHz] for all four probes being calibrated, with a level slowly coming down from 5E^{-10} to 1E^{-12} $[\text{V}^2/\text{Hz}]$.

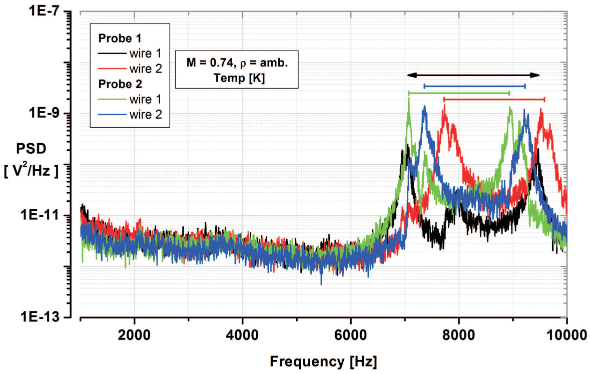

Fig. 23. Power spectral density between 1000 [Hz] and 10000 [Hz] recorded for two probes in the DANTEC calibration unit at Ma=0.74 [-]

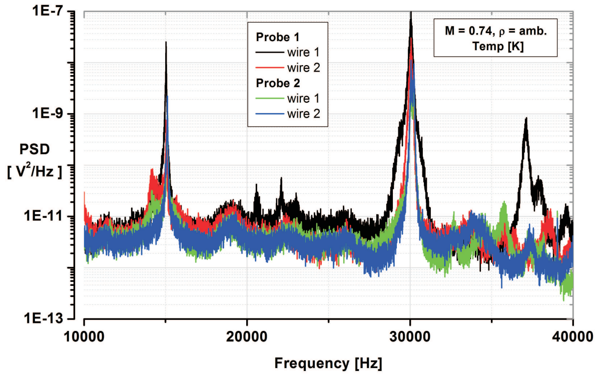

Fig. 24. Power spectral density recorded between 10000 [Hz] and 40000 [Hz] for two probes in the DANTEC calibration unit at Ma=0.74 [-]

The widely smooth spectra are marked by a couple of peaks at about 7000 [Hz] to 9500 [Hz] as well as distinctive peaks at 15000 [Hz] and 30000 [Hz]. They can be traced back to two sources: The 15 [kHz] peak seems to be due to wire vibrations generating a more powerful first harmonic at 30 [kHz]. The pair of peaks (e.g. 7080 [Hz] and 8960 [Hz] for probe 2 and wire 1 was identified to be due to vibrations of the prongs. While the absolute frequency of the peaks is moving for the different wires, their spacing is nearly constant by about 1800 [Hz] with a frequency ratio of 1.25 [-]. Referring to the fixed-beam theory applied to the prongs with their nominal length of 8.35 [mm] and 7.5 [mm] respectively, the expected ratio would be 1.24 [-]. It is worth to note that a difference of 0.1 [mm] in prong length would already cause a change in the vibration frequency of 250 Hertz, though it seems realistic the frequencies to represent the prong's signature. Further analysis of the spectra taken during calibration focused on Mach number effects. It has been detected that for Mach=0.3 [-] the PSD forms a bump between 5 [kHz] and 20 [kHz]. Increasing speed the distinct twin peaks are forming in the 7 [kHz] to 10 [kHz] region while the wire vibrations can only be identified for Mach numbers greater than 0.60 [-]. The twin peaks related to prong vibrations is obviously not shifting in frequency as to be seen in figures 25 and 26.

When testing with the hotwire probes in the empty test section of PETW identical sampling rates and recording periods as for calibration in the DANTEC unit were applied. For each point of the test matrix given in Fig. 6 data were sampled for a series of Mach numbers between 0 [-] and 0.9 [-]. Although the zero-speed case reflects zero rpm of the fan, gas movements in the test section may be due to temperature/density fluctuations as PETW features for cost reasons an external insulation and no perfect thermal equilibrium between the test section and outside the shell could be established. As mentioned before three different overheat ratios 1.8 [-], 2.0 [-] and 2.2 [-] were applied to the hotwires. Not surprisingly, no significant effect of the overheat ratio on the spectrum can be identified over its full range.
To identify tunnel specific behavior in the spectra a comparison has been made between tunnel and calibration

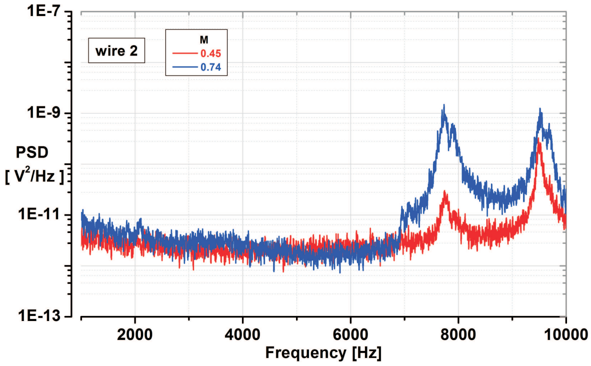

Fig. 25. Mach number effect on PSD between 1000 [Hz] and 10000 [Hz] recorded during calibration using the DANTEC calibration unit

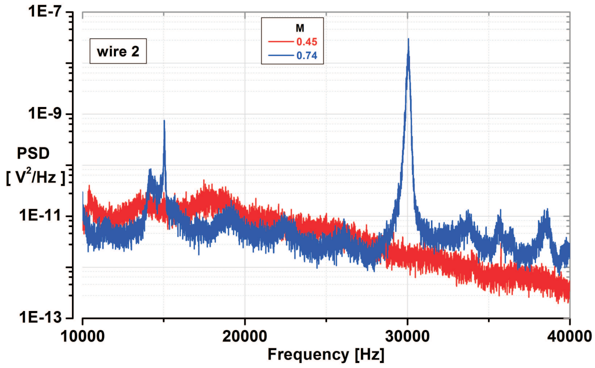

Fig. 26. Mach number effect on PSD between 10000 [Hz] and 40000 [Hz] recorded during calibration using the DANTEC calibration unit

(Figures 27 to 29). Due to the limitations in supply pressure during the hotwire calibration in the DANTEC calibration unit the Mach numbers are not identical (0.74 [-] vs 0.8 [-]) but were nevertheless cross-plotted to compare a status of sensitivity to disturbances. To include the individual response of the wires both wires have been considered. Looking at the spectra, the average level of the PSD in the tunnel is about 1.5 decade higher than the one recorded during calibration. The blade passing frequency (BPF) of the PETW fan is peaking at 3800 Hz. Although the reason has not been found the powerful peaks likely caused by wire vibration at 15 [kHz] and 30 [kHz] cannot be detected in the tunnel spectra. Focusing on the frequency range of 7000 [kHz] to 10000 [kHz] we find the twin peaks already discussed earlier. Although their individual wire related frequency differs they appear perfectly reproduced in the tunnel, hence, the do not represent any flow disturbances generated there. Further on, a peak can be identified in the tunnel only at a frequency of 514 [Hz] which is seen by both wires.

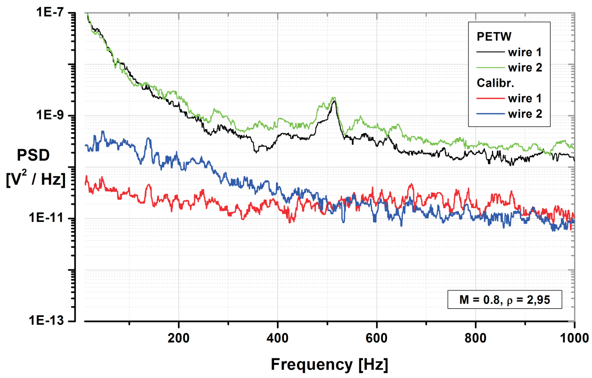

Fig. 27. Comparison of PSD spectra from tunnel and calibration from 0 [Hz] to 1000 [Hz]

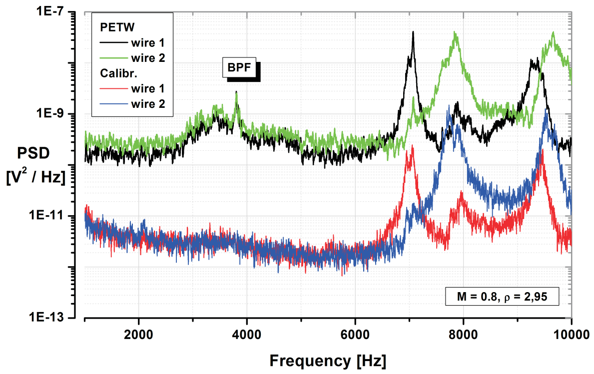

Fig. 28. Comparison of PSD spectra from tunnel and calibration from 1000 [Hz] to 10000 [Hz]

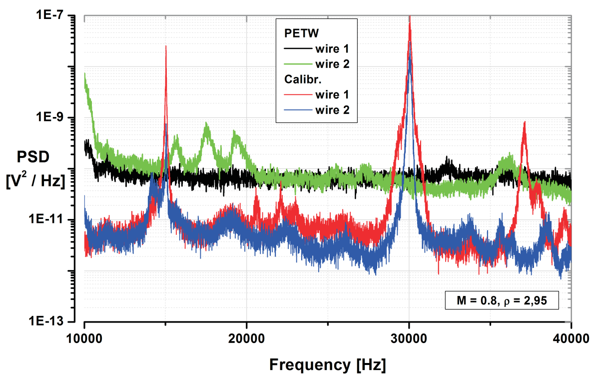

Fig. 29. Comparison of PSD spectra from tunnel and calibration from 10000 [Hz] to 40000 [Hz]

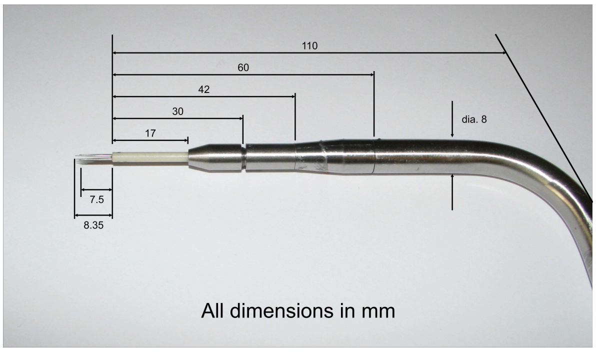

Fig. 30. The modified DANTEC hotwire probe as used in PETW

Figure 30 is providing a close up view of one hotwire probe being used in the tunnel. Due to a non-perfect fit of the sensor's head a gap can be seen at the 30 [mm] downstream location being taped during operation but featuring a flexible joint. Applying again the fixed-beam theory and referencing it to the length of the prong the vibration frequency should be according to

$$f_{prong} \cdot (8.35[mm]/30[mm])^2 = 548[Hz] \tag{9}$$

which is not too far away from the observed value of 514 [Hz].

Now addressing tunnel related effects on the spectra we consider the temperature dependency on specific peaks in the spectra as shown in figures 31 to 33, where the PSD is compared for T=290 [K], 200 [K] and 120 [K]. At the first glance it indicates a dropping PSD level with decreasing temperature for frequencies above 10 [kHz] only. Further analysis reveals no consistent peaks for frequencies below 1 [kHz] and above 10 [kHz] except the one at about 514 Hz. The blade passing frequencies can clearly be identified and decrease as expected with dropping temperature due to the reduced power requirement. Focusing on the 514 [Hz] peak as well as on the twin peaks at about 7 [kHz] and 9 [kHz] they appear shifted to higher frequencies with decreasing temperature. As speed or temperature related correlations like resonances or Strouhal number based effects are dropping frequencies with temperature the only explanation has been found in a dependency on the Young's modulus. For stainless steel it is increasing with decreasing temperature and takes values of 202 [GPa], 211 [GPa] and 214 [GPa] for the gas temperatures of 290 [K], 200 [K] and 120 [K]. Applying again the fixed-beam theory a dependency of frequency to the square root of temperature divided by the cubed prong's length is evident, so decreasing temperature and the according contraction of the prongs both are supporting a trend in the observed direction. The developed theory can similarly be applied to the frequency of the twin peaks. While it is difficult correctly assessing the Eigenfrequency of the prongs itself, it appears easier to evaluate the ratio of these frequencies due to the different length of the prongs, as it is done by equation [9].
Very few fluctuations can be seen for frequencies above 10 [kHz], a range of interest for boundary layer receptivity and transition due to the development of Tollmien-Schlichting waves.

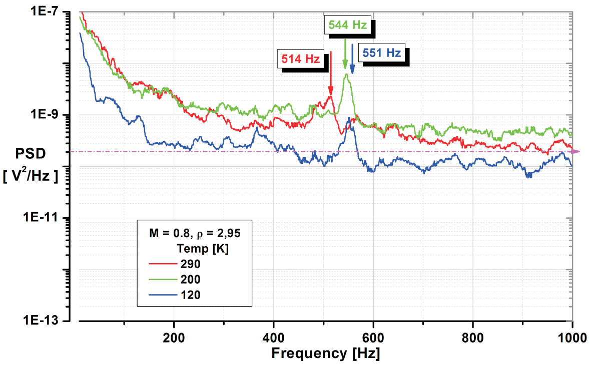

Fig. 31. Comparison of PSD spectra from 0 [Hz] to 1000 [Hz] for different temperatures

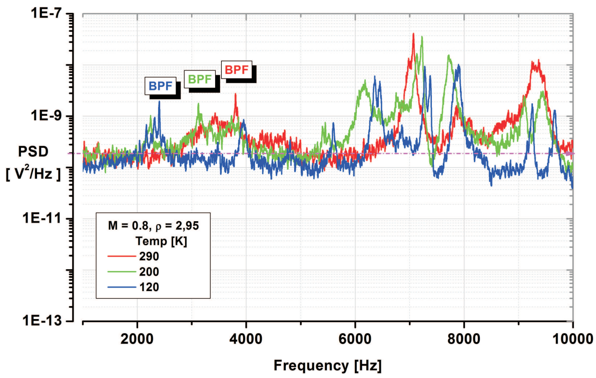

Fig. 32. Comparison of PSD spectra from 1000 [Hz] to 10000 [Hz] for different temperatures

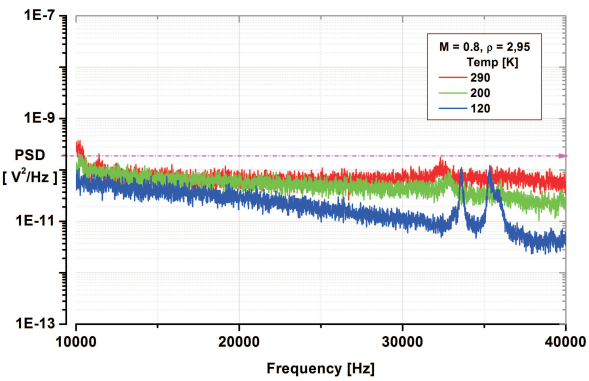

Fig. 33. Comparison of PSD spectra from 10000 [Hz] to 40000 [Hz] for different temperatures

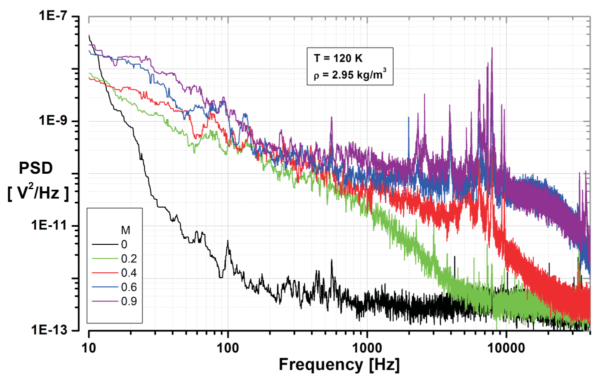

Fig. 34. Mach number effect on power spectral density at cryogenic conditions

Investigating the effect of Mach number at different temperatures we find a very similar behavior for all conditions: relevant effects are clearly visible for frequencies above 500 [Hz]. Here the PSD level is increasing with Mach number. More general, we notice a decrease by about $1\mathrm{E}^{-8}$ to about $1\mathrm{E}^{-13}$ from 10 [kHz] to 40 [kHz]. A typical sample is given in Fig. 34 for a tunnel temperature of 120 K and a few Mach numbers. Data have also be recorded for zero flow speed indicated in Fig. 34 as Ma=0 [-]. Unfortunately, despite zero velocity there may exist temperature or density fluctuations in the absence of a thermal equilibrium. The corresponding graph is characterized by a steep decay of the PSD dropping by about 5 decades over 500 [Hz]. Increasing speeds, the PSD levels start matching the Mach equal zero level at increasing frequencies. For Mach numbers above 0.5 [-] the merge is taking place at frequencies above the measured limit. The spectra are clearly dominated by the prongs' vibrations addressed above. Additionally, Fig. 34 gives the impression of a PSD growth with Mach number in the frequency range below 100 [Hz].

Fluctuations

In a wind tunnel flow unsteadiness may be decomposed into the three independent contributions pressure, entropy and vorticity or density, velocity and total temperature. Operating a hotwire in Constant Temperature Mode (CTA) the recorded voltage signal comprises all sorts of fluctuations. Due to the nature of the CTA only temperature fluctuations may be separated by running at different overheat ratios. Alternatively, V. Lebiga[7] from ITAM in Novosibirsk has demonstrated by operating a single hotwire in constant current mode (CCA) his capability to separate and identify individual fluctuations based on measurements in PETW.
An often applied practice, at least in tunnels operated at ambient conditions, is to neglect any temperature fluctuations and assuming all measured signals being generated by velocity fluctuations only, which might be crude for cryogenic facilities. Subsequently, the dimensionless velocity fluctuation $\widetilde{\mathrm{u}}$ normal to each hotwire may be estimated by

$$Tu_{w1,w2} = (\frac{\widetilde{u}}{\overline{\overline{U}}})_{w1,w2} = 2 \cdot m \cdot \frac{\overline{DC} \cdot AC_{RMS}}{\overline{DC}^2 - DC_0^2} \tag{10}$$

where $\overline{\mathrm{DC}}$ is the time-wise averaged measured voltage DC-signal recorded during wind-on and DC_0 the signal during theoretical wind-off conditions in the tunnel. $\mathrm{AC}_{\mathrm{RMS}}$ refers to the fluctuating AC-voltage component of the measured signal. The $\mathrm{AC}_{\mathrm{RMS}}$ values have been evaluated by integration of the power spectral density versus frequency as e.g. given by Figure 34. To exclude any numerical effects caused by the Fourier Transformation near f=0 [Hz] the spectra have been integrated over the range f=10 [Hz] to f=40000 [Hz].
A widely used definition for the coefficient m is

$$m = \frac{\Delta \log(\rho \cdot U)}{\Delta \log(\overline{DC}^2 - DC_0^2)} \tag{11}$$

Here m represents the slope of a linear fit through the measured data $\log(\rho \cdot \mathrm{U}) = \mathrm{f}(\log(\overline{\mathrm{DC}}^2 - \mathrm{DC}_0^2))$. As demonstrated above a global correction methodology has been developed allowing an approximation of the function Nu = f (Re) for each wire as given in Figure 21 and 22. There the exponent n of the applied allometric power function $\mathrm{Nu}^2 = \mathrm{A} + \mathrm{B} \cdot \mathrm{Re}^{\mathrm{n}}$, an extension of the classical "Freundlich Model", is alternatively equal to 1/m and has been applied to all considered data covering nine combinations of tunnel densities and temperatures, hence, about 900 test points. Subsequently, the overall turbulence level and its axial and lateral components have been evaluated according to equations [12] - [14] and are presented in figures 35, 36 and 37. Fig. 35 representing the overall turbulence level as function of the tunnel Mach number exhibits all turbulence levels to be less than 0.6% maybe even 0.5% if we consider some outliers.

$$Tu_x = \frac{\widetilde{u}}{\overline{\overline{U}}} = \frac{1}{2} \cdot ((\frac{\widetilde{u}}{\overline{\overline{U}}})_{w1} + (\frac{\widetilde{u}}{\overline{\overline{U}}})_{w2})) \tag{12}$$

$$Tu_y = \frac{\widetilde{v}}{\overline{\overline{U}}} = \frac{1}{2} \cdot ((\frac{\widetilde{v}}{\overline{\overline{U}}})_{w1} - (\frac{\widetilde{v}}{\overline{\overline{U}}})_{w2})) \tag{13}$$

$$Tu = \sqrt{\frac{1}{3} \cdot (Tu_x^2 + Tu_y^2 + Tu_z^2)} = \sqrt{\frac{1}{3} \cdot (Tu_x^2 + 2 \cdot Tu_y^2)} \tag{14}$$

While no temperature/density effect can be identified around Ma=0.2 [-] relevant conditions may increase the levels from 0.2% up to maximum values at Mach numbers of 0.9 [-]. The corresponding Fig. 36 using the same data but presenting them as function of Reynolds number, indicated some likely outliers for the high pressure conditions at 200 [K] and 120 [K]. The Reynolds number $\mathrm{Re_d}$ has been defined here as:

$$Re_{d,PETW} = \frac{U \cdot d \cdot \rho_{PETW}}{\eta_{PETW}} \tag{15}$$

Not surprisingly, the contribution of the lateral turbulence levels is low compared to the axial component. As to be seen in Fig. 37 maximum levels appear at the highest Mach number of Ma=0.9 [-] resulting in values of 0.15% not considering the likely outliers already discussed above. It should be noted that despite the clear identification of vibrations caused by components of the hotwire probe, no removal of relevant peaks in the spectra has been applied, hence, the "real" assessed turbulence levels may even be lower than quoted.

Referring to the basic objective of the investigations described in this paper a measurement system has to be developed allowing the future reliable quantitative assessment of fluctuations in ETW supporting an analysis of laminar flow testing as requested by the industry. If we consequently focus on disturbances affecting boundary layer transition we will be more interested in the relevant frequency range defined by Saric[15] for ambient conditions as

$$f = 30 \cdot 10^{-6} \cdot P_\infty \cdot Ma_\infty \cdot 0.117 \cdot 10^{10} \tag{16}$$

where the pressure is to be given in atmospheres. For higher Mach numbers this leads to frequencies in the range of 10 [kHz] to 40 [kHz], hence the gained spectra have been integrated over this range only to get the corresponding $\mathrm{AC_{RMS}}$ values. The calculations reveal overall turbulence levels in the order of 0.1%. Applying Mack's[8] formula developed for flows over flat plates this will lead to N-factors of 8. Transition experiments performed in PETW along the development of temperature sensitive paint for application in cryogenic environment (Cryo-TSP) confirmed this value based on the analysis of the chord-wise transition location. Hence, even better results have to be expected for ETW being designed for high flow quality.

Although testing was performed in the research tunnel PETW only, the number of test conditions (≈ 900) reflects a quite time consuming program. Unfortunately, there could not be found any room for repeats assessing the level of scatter in the data. In opposite to the larger ETW the PETW has no internal insulation thus making it sensitive to an intensified heat transfer when the gas temperature outside the circuit within the surrounding insulation box differs from the one inside the test section. This behavior may be an essential issue when taking the zero Mach number data at cryogenic conditions. Stratification with corresponding density effects or intensified temperature

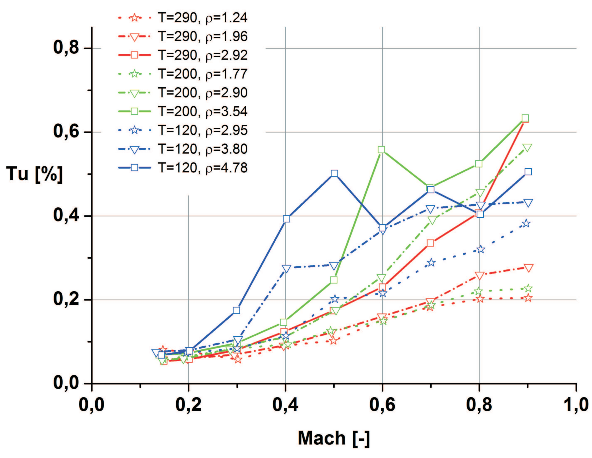

Fig. 35. Overall turbulence level as function of Mach number

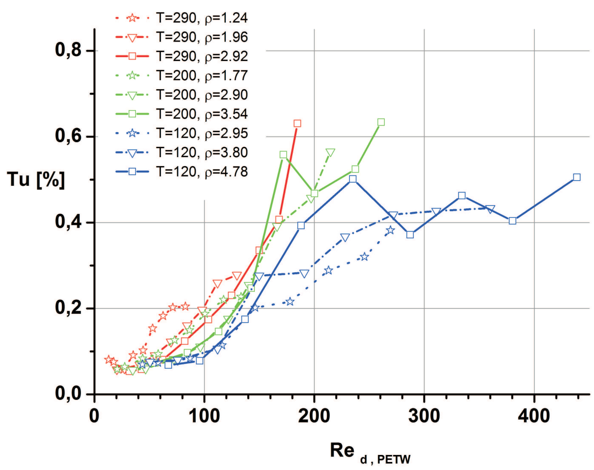

Fig. 36. Overall turbulence level as function of tunnel-wire Reynolds number

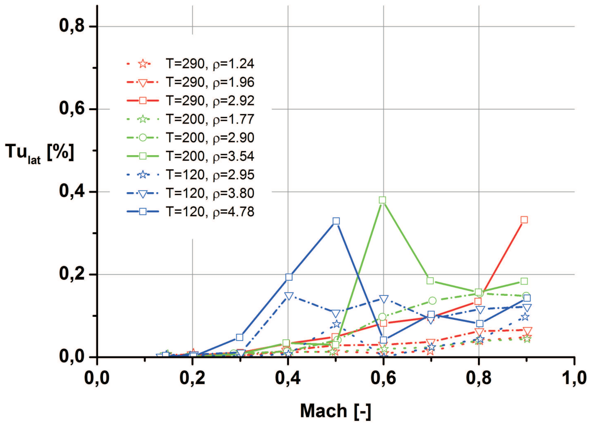

Fig. 37. Lateral turbulence level as function of Mach number

fluctuations might be the consequences to be expected. Nevertheless the performed analysis of the acquired unsteady data is demanding any dependency on density/temperature. In that respect an attempt to filter out something relevant was tried. Reviewing figures 35 and 36 and removing "unlikely" looking points with respect to a Mach or Reynolds number dependency figures 38 and 39 have been achieved. Then, considering the turbulence levels at Ma=0.9 [-] we might see a dependency of density on the turbulence value although the data with a close density ($\rho \approx 2.95[\mathrm{kg/m^3}]$) at Ma=0.6 [-] to Ma=0.9 [-] seem not supporting such a trend. Therefore the plots are flagged with a question mark to underline the speculative character.

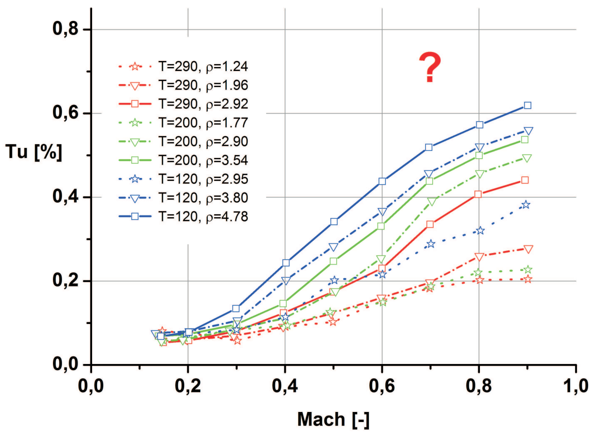

Fig. 38. Author's cleaned overall turbulence level as function of Mach number

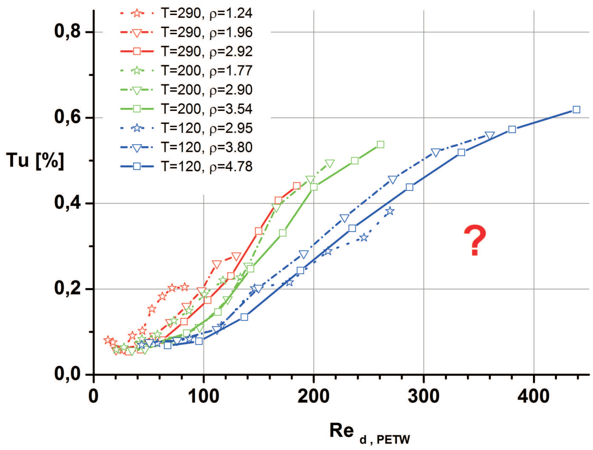

Fig. 39. Author's cleaned overall turbulence level as function of tunnel-wire Reynolds number

E. Survivability

To judge on the survivability of the hotwire probe is very straight forward. Both wires of the probe survived the complete test campaign, including several cool-downs, warm-ups, pressure cycles and varying Mach numbers up to Ma=0.9 [-]. Therefore the survivability of the used probe under pressured and cryogenic conditions can be stated as excellent. One of the principle concerns of using hotwires under such conditions could be eliminated by this test campaigns. Nevertheless it could not be excluded that a particle will hit one or both wires and will destroy the probe. Even therefore it is very helpful to have several calibrated probes for spare.

F. Repeatability

The repeatability of the measurements also plays a major role for the applicability of the measurement technique. Therefore, as already stated, the test program was repeated after two weeks to check the repeatability. Fig. 40 shows the comparison of the initial measurement and the repeat two weeks later. The results is surprising, because

obviously the repeatability for the lower temperatures is very good, while the results at ambient temperature show a significant and unexpected difference. Further investigations show, that the calculated wire resistances at no-wind conditions differ significantly, what is quite unrealistic at the same temperature but very likely a measurement error. Because the calculated wire resistance is used to define the overheat ratio, a wrong wire resistance leads to a false overheat setup. Assuming that the measured wire resistance of the repeat is correct, the result of the initial test at ambient conditions can be corrected for the different overheat value using equation [2]. Applying this correction results in Fig. 41, now showing the same good repeatability for all three temperature levels.
Concluding, it is very important to be confident and accurate in the measurement of all resistances and in the setup of the overheat ratio. If these measurement and settings are performed properly the hotwire provides a very good repeatability in its steady behavior.

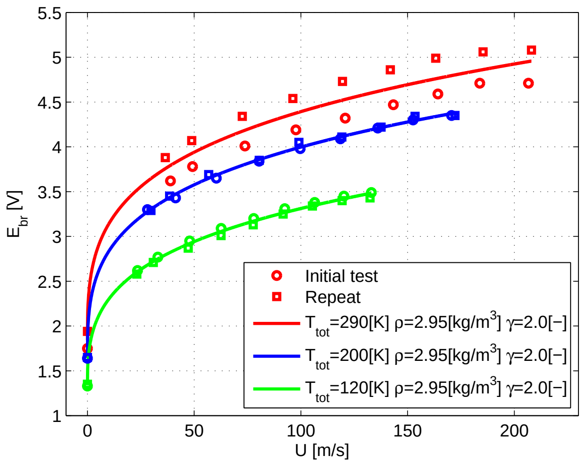

Fig. 40. Repeatability of two measurements with two weeks in between at different temperature levels

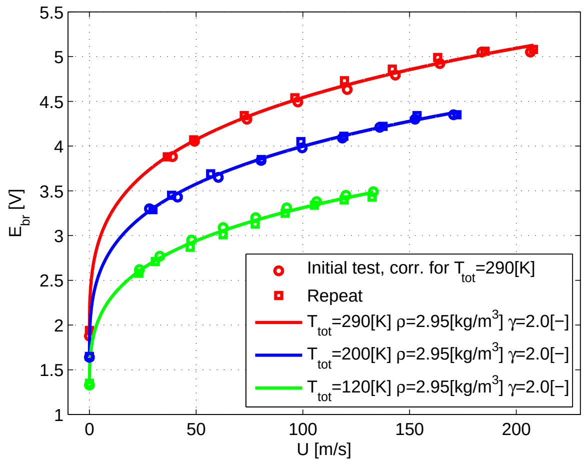

Fig. 41. Repeatability of two measurements with two weeks in between at different temperature levels; Initial measurement for $\mathbf{T_{tot} = 290[K]}$ corrected for different overheat ratio

VI. Conclusion

With respect to an increasing demand for laminar flow testing in the European Transonic Windtunnel (ETW) it is considered essential to assess the flow quality and to identify any disturbance eventually affecting laminar flow development and according boundary layer transition. A promising approach is the use of the hotwire measurement technique for this purpose. As there is little knowledge about reliable application of hotwires in pressurized cryogenic environments a comprehensive tuning of the hardware and the measurement system was performed in ETW's pilot facility PETW to validate the technique before going for an entry in the large facility.
To investigate the applicability of the measurement technique for a cryogenic testing facility an extensive test program with several test objectives was performed. Before focusing on the main goal, the assessment of flow quality, several other aspect have to taken into account, reaching from the simple question of wire survivability, over repeatability to the complex question how to compensate for the different influencing parameters without a costly wire calibration at each test condition. Only if all question have been satisfactorily answered, the hotwire measurement technique can be used in ETW.
The paper presents an overview over the performed test campaign, describing the test objectives, the test setup and concentrating on the test results. Here, the steady hotwire outputs are used to discuss the different varying parameters. The paper shows the influence of velocity, density, temperature and overheat ration on the hotwire results and the possible correction functions for the later three parameters. This correction functions are combined to a global correction function allowing to match the hotwire results of various tunnel conditions to a single calibration taken previous to the test. This procedure is a huge benefit by avoiding time consuming and cost extensive calibration under cryogenic conditions in ETW.
The presented unsteady data clearly show the functionality of the hotwires. Disturbance frequencies like the blade passing frequency could be identified properly. Several observed frequencies could be linked to probe oscillation and frequencies shift tracked back to temperature effects.
In a final step the results of the steady and unsteady analysis have been used to calculate the flow quality represented by the flow fluctuation. Here, the results show only a little dependency from temperature and density variations but are mainly driven by velocity.

Summarizing all results leads to the conclusion that the test campaign was very successful. The hotwire measurement technique is applicable under the harsh conditions of a pressurized and cryogenic testing facility like ETW/PETW. Hence, ETW will continue to establish this technique for future test campaigns and will try to clarify the remaining open questions. The next step will be an application in ETW's large facility, to approve the final outcome of the PETW test campaign: Hotwires in pressurized and cryogenic environment -it works!

References

[1] Archambaud, J.P., *Howire and Pressure Probe Measurements of flow fluctuations in ETW during the Pathfinder Campaign*, ONERA, TELFONA Project D3.1-2b, 2009

[2] Arnal D.; Casalis G.; Houdeville R., *Practical Transition Prediction: Subsonic and Transonic Flows*, RTO-EN-AVT-151

[3] Godden, J.H.M., *Turbulence Measurements in the Cryogenic DNW-KKK Wind Tunnel*, CEAS 2009 European Air and Space Conference, Manchester, 26. - 29. October 2009

[4] Horstmann C.C.; Rose W.C., *Hot-Wire Anemometry In Transonic Flow*, NASA TM X-62,495, 1975

[5] Jorgensen F.E., *How to measure turbulence with hot-wire anemometers - a practical guide*, Dantec Dynamics, 2002

[6] King, L.V., *On the Convection of Heat from Small Cylinders in a Stream of Fluid*, Phil. Trans. of Toy. Soc., Ser. A. Vol. 214, No. 14, p. 373-432, 1914

[7] Lebiga V.;Zinoviev V.;Pak A., *Fluctuation Measurements in Transonic Cryogenic Wind Tunnel*, TELFONA Report: Testing for Laminar Flow for New Aircraft, 2009

[8] Mack, L.M., *Transition Prediction and linear Stability Theory*, AGARD Conf. Proc. No. 224, Paris, France

[9] Michel, U., *Combined Hotwire - Hotfilm Measurements in cryogenic Environment in the PETW*, DLR Institute of Propulsion Technology, Private communication, 1994

[10] Michel U., *Experimental assessment of unsteady flow quantities in wind tunnels with hot-wire anemometry*, DLR Institute of Propulsion Technology, Berlin, 2004

[11] Nagabushana, K.A., *Hot-Wire Calibration in Subsonic/Transonic Flow*, NASA-CR-197725, Langley Research Center, 1994

[12] Nitsche, W., *Strömungsmesstechnik*, Springer Publication Heidelberg, 1994

[13] Owen, F.K.; Owen, A.K., *Measurement and assessment of wind tunnel flow quality*, Progress in Aerospace Science 44, 315-348, 2008

[14] Quix, H., Quest, J., Brzek, C., *Hot-Wire Measurements in Cryogenic Environment*, AIAA-2011-880, 49th Aerospace Science Meeting, Orlando, Fl USA, 4-7 January 2011

[15] Saric W.S.; Reshotko, E., *Review of flow quality issues in wind tunnel testing*,AIAA 98-2613

[16] Spangenberg, W.G., *Heat Loss Characteristics of Hot-Wire Anemometers at various densities in Transonic and Supersonic Airspeeds*, NACA TN 3381, 1955

[17] Stainback, P.C.; Nagabushana, K.A., *Review of Hot-Wire Anemometry Techniques and the Range of their Applicability for Various Flows*, Electronic Journal of Fluids Engineering